Time- and space-integrating spectrum analyzer

Demetri Psaltis and David Casasent

Carnegie-Mellon University, Department of Electrical Engineering, Pittsburgh, Pennsylvania 15213.
Received 28 July 1979.
Sponsored by H. J. Caulfield, Aerodyne Research, Inc.
0003-6935/79/193203-02$00.50/0.

Optical spectrum analysis is a subject of considerable interest. Two-dimensional folded spectrum systems[1–3] and 1-D acoustooptic time-integrating[9] (TI) and space-integrating[5] (SI) systems have been considered as spectrum analyzers. Advanced 2-D versions of these latter two acoustooptic systems[6,7] have recently been described. These triple convolver systems have utilized Fourier kernel factorization and chirp-Z transform methods.[8]

These recent systems still have diverse disadvantages. The bandwidth of the 1-D SI system is large (equal to the bandwidth of the input transducer); however, the frequency resolution is low (inversely proportional to the time aperture of the input transducer). The 2-D SI systems have good frequency resolution, but their bandwidth is limited by the real-time and reusable 2-D spatial light modulator required. Conversely, 1-D TI systems exhibit excellent frequency resolution, but their bandwidth is limited. Although the 2-D TI systems provide an increased bandwidth, this is always less than the bandwidth of the input transducer.

In this Communication, we describe and analyze a 2-D combined TI and SI spectrum analyzer that realizes the best features of the above systems. This system has a large bandwidth (equal to the bandwidth of the input transducer; 1 GHz is possible[9] and an excellent frequency resolution (equal to the reciprocal of the detector integration time t_0).

The principle of operation of this time- and space-integrating spectrum analyzer is best described with reference to Fig. 1. The P_1-L_1-P_2 portion of this system is a 1-D SI processor. When the proper temporal and spatial modulation is introduced at P_2, TI processing (P_2-P_3-P_4) can be applied to the output in the orthogonal direction; this produces an output folded spectrum display with a vertical fine-frequency axis $\hat{y}$ and a coarse-frequency horizontal axis $\hat{x} = \omega_x \lambda f_L / 2\pi$. For simplicity, the single-sideband filtering section of the system and the imaging objects are omitted, and 1:1 imaging is assumed. Only an acoustooptic schematic is shown, although realizations using SAW, CCD, and other technologies are also possible. Heterodyne detection of the output of such a system is also possible and is discussed elsewhere.[10]

Let us now consider a detailed description of the system in Fig. 1. When the acoustooptic line (AO-1) at P_1 is illuminated with the collimated laser beam, the 1-D Fourier transform of the input signal $s(t)$ is produced spatially at P_2 as in a conventional SI system. At P_2 we obtain

$$U_2(\omega_x,t) = \int_{-\infty}^{\infty} s(x - vt)\Pi(x/d_1) \exp(-j\omega_x x)dx, \qquad (1)$$

where $\omega_x = 2\pi x_2/\lambda f_L$ = spatial frequency,
v = acoustic velocity,
f_L = focal length of L_1,
$\Pi(x/d_1)$ = window function of the P_1 transducer, and
d_1 = aperture width at P_1.

For the case of a single input spatial frequency ω_0 (or temporal frequency $w_0 v$), the pattern at P_2 is

$$U_2(\omega_x,t) = \exp(-j\omega_0 vt) \operatorname{sinc}[d_1(\omega_x - \omega_0)]. \qquad (2)$$

From Eq. (2), we see that the input signal frequency can be found from the location of the peak of the P_2 light distribution (at $\omega_x = \omega_0$). Unfortunately, the broad main lobe width ($1/d_1$) of this P_2 pattern limits the frequency resolution in P_2. However, improved system performance is possible if we properly use the temporal modulation [first term in Eq. (2)] at frequency $w_0 v$ present in the spatial P_2 pattern.

To utilize the signal information, we first realize that the $w_0 v$ temporal frequency can lie anywhere within the bandwidth of the input AO cell. This large bandwidth is generally more than a normal TI system can utilize. However, we can view the P_2 pattern as a coarse-frequency spatial spectrum (with coarse spatial frequency resolution equal to the coarse temporal bandwidth v/d_1) and realize that we need only accurately determine the location of the input frequencies within the main lobe of the sinc function in Eq. (2). To utilize a TI processor on this P_2 output, we first heterodyne the signals at points separated by $1/d_1$ along ω_x in P_2 to baseband. This can be accomplished by the linear array of temporal modulators shown in Fig. 1. These modulators are located at spatial frequencies ω_{xn} along the ω_x axis and have temporal frequencies $\omega_{nx} v = nv/d_1$.

With the transmittance of the 1-D mask at P_2 described by

$$t_2(\omega_x,t) = \sum_n \exp(jnvt/d_1)\Pi[(\omega_x - n/d_1)d_1], \qquad (3)$$

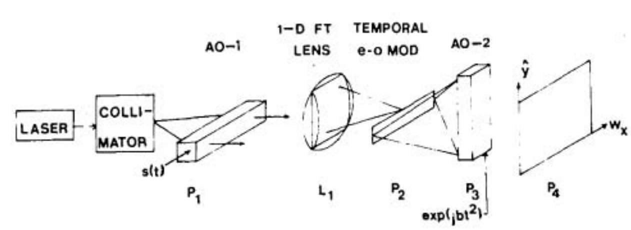

Fig. 1. Time- and space-integrating spectrum analyzer using a linear temporal modulator.

the light distribution leaving P_2 is $U_2(\omega_x,t)t_2(\omega_x,t)$. We now form the 1-D Fourier transform of U_2t_2 with respect to time at P_4 using a chirp-Z optical Fourier transform system. This Fourier transform is formed by focusing P_2 onto P_3, smearing P_2 vertically at P_3, and imaging P_2 horizontally at P_4. An acoustooptic cell (AO-2) at P_3 is fed with a chirp signal $\exp(jbt^2)$. At P_4, we find

$$U_4(\omega_x,\hat{y}) = \mathrm{sinc}[d_1(\omega_x - \omega_0)]\,\mathrm{sinc}[(bt_0/v) \times (\hat{y} - \omega_0 v^2/b + n_0 v^2/bd_1)]. \quad (4)$$

In obtaining Eq. (4), we have retained only the single $n = n_0$ term in the summation in Eq. (3) that produces a baseband signal. Assuming that both AO lines have the same aperture d_1, then $y_{max} = d_1$, the maximum temporal frequency in the basebanded signal, is $by/v = bd_1/v$, and this must equal v/d_1, from which we find the chirp waveform constant to be

$$b = v^2/d_1^2. \quad (5)$$

In Eq. (4), t_0 is the integration time of the detector at P_4. If we choose t_0 to be an integer number N of input SI system time windows,

$$t_0 = Nd_1/v, \quad (6)$$

Eq. (4) becomes (for a single-frequency ω_0 input signal)

$$U_4(\omega_x,\hat{y}) = \mathrm{sinc}[d_1(\omega_x - \omega_0)]\,\mathrm{sinc}[(N/d_1) \times (y - \omega_0 d_1^2 + n_0 d_1)]. \quad (7)$$

With a wide area modulator for AO-2, we can also achieve the desired functions by imaging P_2 onto P_3 and onto P_4. From Eq. (7), we see that the sinc distribution of the output peak is of width $1/d_1$ in the ω_x coarse-frequency axis and of width d_1/N in the imaging or $\hat{y}$ axis. This latter width of the peak in $\hat{y}$ is $1/N$ of the width d_1 of the entire $\hat{y}$ aperture. This d_1 aperture in $\hat{y}$ represents a bandwidth of v/d_1. Thus the P_4 distribution is a folded spectrum with a coarse-frequency ω_x axis and a fine-frequency $\hat{y}$ axis. Along ω_x, the location of the peak for an input spatial frequency ω_0 is proportional to ω_0, whereas the location of the peak along $\hat{y}$ is proportional to the heterodyned frequency $\omega_0 - n_0/d_1$ and hence to the fine frequency within the coarse-frequency bin of width v/d_1 centered at ω_0.

Progress on integrated electrooptic temporal modulator arrays of the type needed at P_3 of Fig. 1 are encouraging.[11] However, an alternate system topology exists as shown in Fig. 2. To understand this system we simply rewrite Eq. (3) as (ignoring a multiplicative v/d_1 constant on the left)

$$\sum_m \exp(j2\pi mvt/d_1) = \sum_n \delta(t - nd_1/v). \quad (8)$$

In this form, the suggested implementation in Fig. 2 results,

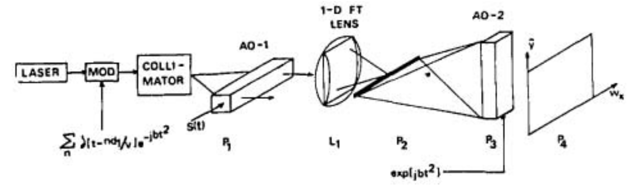

Fig. 2. Time- and space-integrating spectrum analyzer using a pulse-modulated source.

in which the laser source is time sequentially pulse modulated as shown. In this embodiment, all oscillator frequency signals appear at all spatial locations in ω_x in plane P_2. This results in basebanded signals at center frequencies v/d_1, $2v/d_1$, etc. at all spatial locations ω_x. Since the largest temporal frequency produced by the chirp-Z optical Fourier transform system is v/d_1, all signals except the basebanded one will integrate to zero at P_4, and the same resultant folded spectrum output occurs.

Although component research remains before the system in Fig. 1 can be realized and light level losses will result when the system in Fig. 2 is used, hybrid SI-TI approaches to high-bandwidth and resolution spectrum analyzers appear preferable to other methods. Other approaches to high-bandwidth and frequency resolution optical spectrum analyzers require one of the signals to be scanned and result in a cumulative output bias level.[10] The system described appears to achieve the full bandwidth and frequency resolution possible without such difficulties.

The support of this research by the Office of Naval Research on a cooperative joint contract between NOSC and CMU is gratefully acknowledged.

References

1. C. E. Thomas, Appl. Opt. **5**, 1782 (1966).
2. D. Casasent and R. Kessler, Opt. Eng. **16**, 402 (1977).
3. J. Anderson, H. Brown, and B. Markevitch, Proc. SPIE **180**, in press (1979).
4. R. Sprague and C. Koliopoulos, Appl. Opt. **15**, 89 (1976).
5. R. Sprague, Opt. Eng. **16**, 467 (1977).
6. T. Turpin, Proc. SPIE **154**, 196 (1978).
7. P. Kellman, in *Proceedings of 1978 International Optical Computer Conference* (IEEE, New York, 1978), 78CH1305-2C, p. 91.
8. J. Speiser and H. Whitehouse, Naval Ocean Systems Center, NUCTN 1355R (1974).
9. D. Hecht, Proc. SPIE **90**, 148 (1976).
10. T. Bader, Appl. Opt. **18**, 1668 (1979).
11. G. Aitken and A. Kidd, Appl. Opt., **17**, 3884 (1979).

A REMINDER

Authors submitting Rapid Communications for publication must remember to include a letter from their institution agreeing to honor the publication charge. Otherwise publication will be delayed— and the whole idea of this section of Letters to the Editor is defeated.